JACS
JOURNAL OF THE AMERICAN CHEMICAL SOCIETY

Communication

pubs.acs.org/JACS

Efficient Photochemical Dihydrogen Generation Initiated by a Bimetallic Self-Quenching Mechanism

Matthew B. Chambers, Daniel A. Kurtz, Catherine L. Pitman, M. Kyle Brennaman, and Alexander J. M. Miller*

Department of Chemistry, University of North Carolina at Chapel Hill, Chapel Hill, North Carolina 27599-3290, United States

Supporting Information

ABSTRACT: Artificial photosynthesis relies on coupling light absorption with chemical fuel generation. A mechanistic study of visible light-driven H_2 production from $[Cp^*Ir(bpy)H]^+$ (**1**) has revealed a new, highly efficient pathway for integrating light absorption with bond formation. The net reaction of **1** with a proton source produces H_2, but the rate of excited state quenching is surprisingly acid-independent and displays no observable deuterium kinetic isotopic effect. Time-resolved photoluminescence and labeling studies are consistent with diffusion-limited bimetallic self-quenching by electron transfer. Accordingly, the quantum yield of H_2 release nearly reaches unity as the concentration of **1** increases. This unique pathway for photochemical H_2 generation provides insight into transformations catalyzed by **1**.

Light-driven production of dihydrogen (H_2) from low energy proton sources is a central transformation in the continued development of solar energy storage technologies.[1−4] The most advanced solar fuels devices are semiconductor photoelectrodes comprised of separate light absorption, charge separation and catalyst components.[3] These multicomponent systems can be difficult to prepare, inefficient in mediating interfacial charge transfer, and operationally unstable.[2,4] Molecular approaches to photochemical H_2 generation also typically involve multicomponent mixtures that feature photosensitizers, redox mediators, and catalysts.[5−7]

A simpler approach would utilize a single molecular photocatalyst that absorbs light and mediates H_2 formation. One class of single-component photocatalyst is Nocera's dirhodium platform, in which photochemical X_2 elimination followed by reaction with hydrohalic acids generates metal hydrides that can photochemically produce H_2.[7−9] We have pursued a strategy in which a metal hydride is generated electrochemically at mild potentials and then absorbs visible light to release H_2. This molecular photoelectrocatalyst strategy remains relatively unexplored, however, and development is limited by the lack of molecular complexes that photochemically generate H_2 with high efficiency.[9] Tightly integrating electrochemical and photochemical steps into a single tunable molecular photocatalyst could improve efficiency relative to current multicomponent systems.

We recently reported the first example of H_2 evolution by molecular photoelectrocatalysis.[10] The catalyst $[Cp^*Ir(bpy)Cl]^+$ (**2-Cl**) produces H_2 from neutral water near the H^+/H_2 thermodynamic potential with high Faradaic efficiency and external quantum efficiency (~10%).[10] The light-absorbing intermediate is the metal hydride $[Cp^*Ir(bpy)H]^+$ (**1**), synthetically accessible in high yield and capable of quantitative production of H_2 upon illumination in water or acetonitrile (CH_3CN) in the presence of acids (Scheme 1).[10,11] Hydride **1** has a rich history in photochemical catalysis and is a key intermediate in light-driven water−gas shift, formic acid dehydrogenation, and proton transfer processes.[12−15] Even in the dark, **1** is a thermal catalyst for a wide range of hydrogen transfer reactions.[16,17,18]

Scheme 1. Molecular Photoelectrochemical H_2 Evolution

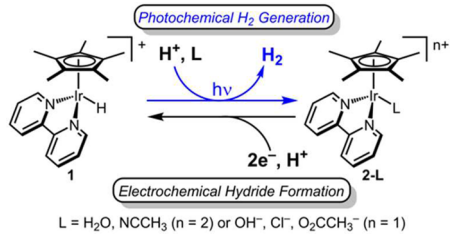

Despite the prominent photocatalytic role of monohydride **1**, little is known about the mechanism of photochemical H_2 release.[10,11] In contrast to dihydride complexes that release H_2 through well-understood reductive elimination photoprocesses, light-driven H_2 release from monohydride complexes is rare and mechanistically ill-defined.[9,19,20] Scheme 1 shows net hydride/proton coupling to release H_2, which could occur via a concerted hydride ion transfer, stepwise electron/hydrogen atom transfer, or a three-step sequence of proton and electron transfers. More broadly, the nature of the H_2 release process remains an enduring mechanistic question for all monohydride photocatalysts and electrocatalysts: hydrides most commonly release H_2 by reaction with a proton source, but rare examples of bimetallic coupling have also been proposed.[21−24] We embarked on a mechanistic study of H_2 release from **1** to reveal the origins of its remarkable photoefficiency and provide guiding principles for the development of future photocatalysts.

Indications of an unexpected bimetallic mechanism were uncovered while studying photoelectrocatalytic H_2 evolution in aqueous media. The chloride complex **2-Cl** was prepared as previously described and the rate of H_2 evolution was analyzed by chronoamperometry (CA).[10] As the catalyst concentration was varied from 0.25 mM to 1 mM, the observed rate constant for H_2 evolution catalysis exhibited an unexpected dependence on

Received: August 19, 2016
Published: September 27, 2016

DOI: 10.1021/jacs.6b08701
J. Am. Chem. Soc. 2016, 138, 13509−13512

Scheme 2. Possible Pathways of H_2 Generation from 1

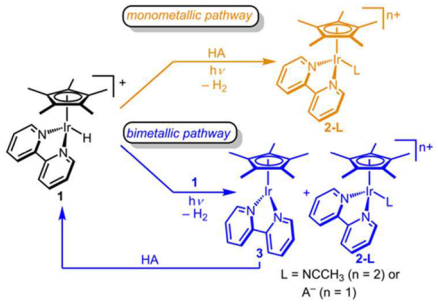

catalyst concentration. If the reaction is first order in catalyst, rate constants determined using the electroanalytical equations of Nicholson and Shain should not vary as a function of catalyst concentration.[25] The observed linear dependence (Figure S2) instead suggests that the process is second order in catalyst.

To further probe the mechanism of photochemical H_2 release from **1**, we isolated the hydride and examined its excited state reactivity in CH_3CN. In prior studies in CH_3CN, we established that **1** cleanly releases H_2 with organic acids and characterized some relevant thermochemical properties, without exploring the detailed mechanism and kinetics.[11] In this work, CH_3CN solvent supports the use of well-defined organic acids with tunable pK_a values and makes possible labeling experiments that would be hampered by H/D exchange in water.[12,18d]

Visible light illumination of **1** in CH_3CN containing excess acetic acid (CH_3CO_2H) cleanly generates H_2 and $[Cp^*Ir(bpy)(O_2CCH_3)]^+$ (**2-O_2CCH_3**). The reaction is easily monitored by ^1H NMR or UV−vis spectroscopy, and the yield of H_2 is quantitative by gas chromatography.[11] Scheme 2 outlines the two broad photochemical H_2 release pathways considered. In the monometallic pathway, the iridium hydride excited state reacts with a proton donor. In the bimetallic pathway, two iridium hydrides react to afford H_2 along with **2-L** and $Cp^*Ir(bpy)$ (**3**),[26,27] which are favored over unstable Ir(II) species.[28,29] Protonation of **3** regenerates one equivalent of **1.**

A labeling study was performed to differentiate between the monometallic and bimetallic pathways of Scheme 2. In the presence of a deuterated acid, photolysis of unlabeled **1** would produce HD via the monometallic pathway, whereas H_2 would be produced via the bimetallic pathway. Photolyses of **1** were performed in CD_3CN with a 10-fold excess of CD_3CO_2D and the isotopic distribution of dihydrogen was monitored periodically by ^1H NMR spectroscopy. Substantial quantities of both HD and H_2 were detected over the 30 min needed to reach completion (Figure 1). The inset of Figure 1 reveals an initial burst of H_2 in the first minute, followed by formation of HD (before both solvated gases are lost to the headspace). On the time scale of these experiments, H/D exchange in the dark is negligible (Figure S12). The observation of H_2 suggests that a bimetallic pathway is operative.

At the end of the reaction, the acetate complex **2-O_2CCH_3** is the sole product. During the course of the reaction, however substantial amounts of $[Cp^*Ir(bpy)(NCCH_3)]^{2+}$ (**2-$NCCH_3$**) were also observed, in accord with the bimetallic pathway of Scheme 2. Although not observed, intermediate **3** could be protonated by CD_3CO_2D to afford an iridium deuteride.[12,26] Continued irradiation would lead to coupling between Ir−H and Ir−D, accounting for the HD observed at later times. Consistent with this hypothesis, the hydride resonance of **1** diminishes twice as fast as the Cp* resonances (Figure S8) due to the generation of 1 equiv of $[Cp^*Ir(bpy)D]^+$ (**1-D**) for each equiv of H_2. Further

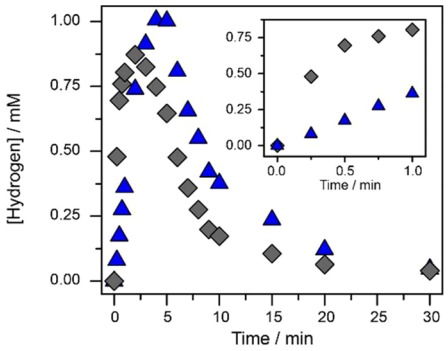

Figure 1. Concentration of H_2 (▲) and HD (◆) detected by ^1H NMR spectroscopy during the photolysis of 11.5 mM of **1** and 100 mM of CD_3CO_2D in CD_3CN with 460 mn light. Inset shows the first 1 min. H_2 concentration corrected for thermal population of para-H_2.[31]

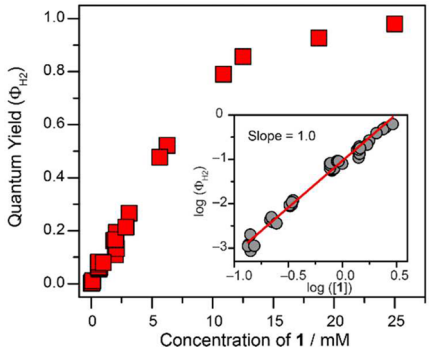

Figure 2. Quantum yield at various concentrations of **1** with excess CH_3CO_2H in CH_3CN solution (443 nm at a flux of 1.9×10^{-6} mol of photons min^{-1} cm^{-2}). Inset: $\log(\Phi_{H2})$ vs $\log([\mathbf{1}])$ up to 5 mM.

evidence against the monometallic pathway comes from reactions varying the acidity of the proton source. The initial rate of conversion of **1** in the presence of $[DNEt_3]^+$ (pK_a = 18.8 in CH_3CN)[30] was essentially the same as the initial rate of conversion in the presence of CD_3CO_2D (pK_a = 23 in CH_3CN).

If the bimetallic process is rate-determining, the quantum yield of H_2 formation (Φ_{H2}) should depend on the concentration of **1**. Initial rates of H_2 formation from CH_3CN solutions of **1** and an organic acid illuminated with a 443 nm LED light source were obtained by monitoring the reaction progress by UV−vis spectroscopy. Quantum yields were calculated by dividing the initial rates of H_2 formation by the photon flux.[32]

Figure 2 shows that Φ_{H2} increases dramatically with increasing concentrations of **1**. Remarkably, illuminating solutions above 19 mM in **1** gives $\Phi_{H2} > 0.93$. Hydride **1** must be fulfilling a role beyond light absorption that facilitates efficient light-to-fuel energy conversion. Plotting $\log(\Phi_{H2})$ vs $\log([\mathbf{1}])$ (Figure 2 inset) reveals a slope of 1. A photochemical reaction that is first order in the light absorber **1** should have a quantum yield that is independent of the concentration of **1**. The observed concentration dependence suggests that the reaction is second order in **1**.

To interrogate specifically the excited-state reactivity of **1**, we turned to photoluminescence spectroscopy. Excitation of **1** at 443 nm at 298 K yields **1***, a triplet excited state that exhibits a broad, featureless emission peak with a maximum at 708 nm.[11,33] Addition of acid led to no observable decrease in emission intensity. On the contrary, emission quenching was evident as the concentration of **1** increased, with a Stern−Volmer quenching constant (K_{SV}) of 230 M^{-1} (Figure S28).

DOI: 10.1021/jacs.6b08701
J. Am. Chem. Soc. 2016, 138, 13509−13512

Table 1. Excited-State Lifetimes and Self-Quenching Constants Determined by Stern–Volmer Analysis[a]

sample[a]	τ_o (ns)	K_{SV} (M^{-1})	k_q (M^{-1} s^{-1})
$[Cp^*Ir(bpy)H]^+$ + acid[b]	103	360	3.5×10^9
$[Cp^*Ir(bpy)H]^+$	98	370	3.8×10^9
$[Cp^*Ir(bpy)D]^+$[c]	118[d]	480	4.0×10^9

[a]Ir concentrations between 0.1 and 1 mM evaluated in CH_3CN with 100 mM $[Bu_4N][PF_6]$.[32] [b]Samples run with 50 mM CH_3CO_2H. [c]Synthesis of isotopically labeled **1-D** (88% D by ^1H NMR). [d]Longer τ_o is in accord with excitation from *d*-orbital with Ir–D character.[35]

Time-resolved photoluminescence spectroscopy can provide more detailed information on the nature of emission quenching. We set out to measure changes in luminescence lifetime (τ) of **1*** under various reaction conditions. Consistent with the steady-state behavior, τ was invariant with respect to CH_3CO_2H concentration (Figure S37), suggesting that the acid does not react directly with the excited state **1***. The lifetime decreased significantly with increasing [**1**] in the presence of a constant concentration of CH_3CO_2H (Figure S34). The decrease in τ is indicative of dynamic self-quenching and indicates that the bimetallic process directly involves excited state **1***.

Self-quenching rate constants were determined via Stern–Volmer analysis, after estimating the intrinsic lifetime of **1*** if it were in the absence of quencher (τ_o) by extrapolating the relationship between the lifetime and [**1**] to infinite dilution (Figures S34 and S35).[34] The results of Stern–Volmer analysis are presented in Table 1. In the presence of acid, **1** features a self-quenching rate constant ($k_q = 3.5 \times 10^9$ M^{-1} s^{-1}) nearing the diffusion limit. In the absence of acetic acid, the quenching behavior is essentially identical, $k_q = 3.8 \times 10^9$ M^{-1} s^{-1}.

Kinetic isotope effect (KIE) studies indicate that no Ir–H bond breaking occurs during self-quenching. Deuterium-labeled **1-D** has a self-quenching rate constant of 4.0×10^9 M^{-1} s^{-1}, providing a KIE of 1.0(1) (Table 1). This experiment rules out photochemical Ir–H homolysis to produce free H·, which has been observed previously.[9] The absence of free H· is further supported by the limiting value $\Phi_{H2} = 1$ and the lack of HD formation during photolysis of **1** and CD_3CO_2D in CD_3CN.

Self-quenching without bond-breaking can be observed in triplet–triplet annihilation.[36] To probe for a bimolecular reaction involving two equivalents of **1***, quantum yields were measured at constant concentrations of **1** and CH_3CO_2H with a variable photon flux. Only a slight decrease in Φ_{H2} with increasing photon flux is apparent, ruling out quenching through the interaction of two excited state species. Furthermore, the lifetime of **1*** is invariant with respect to the intensity of the excitation pulse (1–6 mJ, Figure S43). The combined time-resolved luminescence data are fully consistent with bimetallic self-quenching by electron transfer between **1*** and **1**. Though self-quenching has been observed in other organometallic complexes, it has not been coupled with H_2 release or other chemical bond formation.[34,37,38]

Scheme 3 depicts a mechanism for photochemical production of H_2 from **1** that is consistent with all of the experimental data. Photoexcitation of **1** affords metal-to-ligand-charge-transfer (MLCT) triplet excited-state **1***, which is quenched by another molecule of **1** via diffusion-controlled electron transfer. As the concentration of **1** increases, the rate of electron transfer increases, eventually outcompeting other decay pathways to enable quantitative photon-to-fuel efficiency. Electron transfer would produce highly reactive hydrides $Cp^*Ir(bpy)H$ (**4**) and $[Cp^*Ir(bpy)H]^{2+}$ (**5**), which could rapidly couple by hydrogen atom

Scheme 3. Proposed Mechanism of H_2 Formation from 1

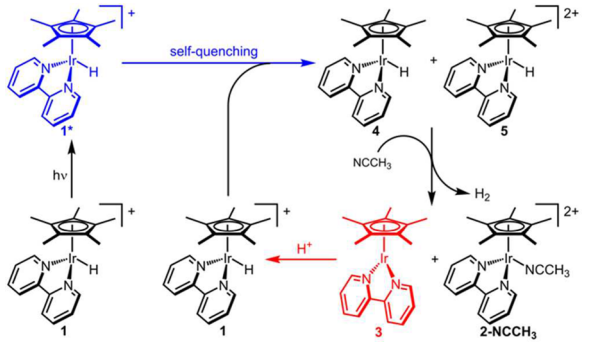

transfer to generate H_2 along with **3** and **2-NCCH$_3$**. Protonation of **3** regenerates **1**, accounting for the overall 1:1 stoichiometry of **1**:H^+. In the absence of acid, the major product is a previously reported bridging iminoacyl derived from CH_3CN, which is formed with H_2 and other Ir-containing species (Figure S13).[11]

The photochemical process is rate-determining for H_2 release due to the low concentrations of **1*** maintained during steady-state photolysis. Consistent with protonation occurring after the rate-determining process, Φ_{H2} was independent of acid strength (CH_3CO_2H vs $[HNEt_3]^+$) during steady-state photolyses. A KIE of 1.0(1) was obtained upon comparison of Φ_{H2} for **1** and **1-D** in the presence of 50 mM CH_3CO_2H.

In an effort to facilitate electron transfer between two cationic species **1*** and **1**, the supporting electrolyte $[Bu_4N][PF_6]$ was added to the solvent. The lifetime of **1*** decreases as the concentration of $[Bu_4N][PF_6]$ increases, indicating more efficient self-quenching and supporting the proposed mechanism. If electrolyte accelerates the rate-determining step, the overall quantum yield for H_2 release under steady-state photolysis should increase as well. Compared to the original conditions, Φ_{H2} doubled when CH_3CN solutions of 0.1 M $[Bu_4N][PF_6]$, 0.55 mM **1**, and excess CH_3CO_2H were photolyzed (Figure S22).

A self-quenching pathway for H_2 evolution is unprecedented, to our knowledge. To assess the plausibility of this new mechanism, self-quenching H_2 evolution was analyzed from a thermodynamic perspective. The driving force for electron transfer between **1*** and **1** (eq 1) can be estimated based on the energy difference between the triplet excited state and the singlet ground state (ΔG_{ST}) and the redox properties of **1**.[32] A range of $47 < \Delta G_{ST} < 52$ kcal/mol is estimated based on variable-temperature emission spectra.[32] Cyclic voltammograms of **1** exhibit a quasi-reversible reduction ($E_{1/2} = -1.80$ V vs $Fc^{+/0}$) that becomes less reversible at slow scan rates.[29] An irreversible oxidation feature is also observed; some reversibility apparent at scan rates beyond 100 V/s provides an estimate of $E_{1/2} = 0.50$ V vs $Fc^{+/0}$.

The self-quenching reaction of eq 1 is nearly thermoneutral ($\Delta G^\circ = 3 \pm 2$ kcal/mol), with oxidation and reduction potentials for **1*** estimated as $+1.6 \pm 0.1$ V and -0.34 ± 0.11 V, respectively. Endergonic excited-state electron transfers are not uncommon, and efficient rates have been observed in organometallic systems when unfavorable electron transfer ($\Delta G^\circ = +7$ kcal/mol) is followed by an irreversible chemical step.[39] Thus, self-quenching will be thermodynamically viable if the subsequent H_2 generation proceeds with significant driving force.

$$\mathbf{1}^* + \mathbf{1} \rightarrow Cp^*Ir(bpy)H + [Cp^*Ir(bpy)H]^{2+} \quad (1)$$

$$Cp^*Ir(bpy)H + [Cp^*Ir(bpy)H]^{2+} \rightarrow \mathbf{3} + \mathbf{2} - \mathbf{L} + H_2 \quad (2)$$

DOI: 10.1021/jacs.6b08701
J. Am. Chem. Soc. 2016, 138, 13509–13512

The H−H coupling process (eq 2) was analyzed by a separate thermochemical cycle. Homocoupling of **4** and **5** would directly produce **3** and **2-L**. Heterocoupling, with **4** delivering H^- and dicationic **5** delivering H^+, would generate 2 equiv $[Cp^*Ir^{II}(bpy)]^+$. The Ir(II) species would disproportionate to the same products **3** and **2-L**,[28] so the thermochemistry of the two coupling routes is identical. The homocoupling pathway was used to assess eq 2 using the bond dissociation free energy (BDFE) values of **4** and **5**.[32] Based on the CV of **1** and the previously reported hydricity of **1** (62 kcal/mol),[11] very weak BDFEs are established for **4** (45 kcal/mol) and **5** (25 kcal/mol). Coupling to release H_2 is favorable by more than 33 kcal/mol.

The combined kinetic and thermodynamic analyses bring clarity to decades of photochemistry involving $[Cp^*Ir(bpy)H]^+$ (**1**). Hydride **1** generates H_2 through an unprecedented, extremely efficient photochemical pathway initiated by self-quenching electron transfer. We hypothesize that the nearly perfect photon-to-fuel efficiency of **1** is a consequence of quenching the excited state via electron transfer, a process that is typically efficient. The second-order kinetics can be harnessed to produce H_2 in bulk with nearly perfect quantum efficiency. Surprisingly, the role of the acid source is simply to regenerate 1 equiv of **1** after H_2 release, which could lead to benefits such as pH-independent H_2 evolution catalysis. Self-quenching also poises the system for bimetallic H_2 evolution, which is rarely observed in photochemical or electrochemical catalysis. A catalyst that operates by efficient self-quenching offers an exciting new direction in photochemical H_2 evolution, circumventing the need for separate photosensitizers and redox mediators and enabling highly efficient photo(electro)catalysis.

■ ASSOCIATED CONTENT

Supporting Information

The Supporting Information is available free of charge on the ACS Publications website at DOI: 10.1021/jacs.6b08701.

Experimental details (PDF)

■ AUTHOR INFORMATION

Corresponding Author

*ajmm@email.unc.edu

Notes

The authors declare no competing financial interest.

■ ACKNOWLEDGMENTS

This work was supported by the Division of Chemical Sciences, Geosciences & Biosciences, Office of Basic Energy Sciences of the U.S. Department of Energy through Grant DE-SC0014255. A fellowship to C.L.P. was supported by the Royster Society of Fellows. This work made use of the Photon Technology, Inc. Quantamaster 4SE-NIR5 and Edinburgh FLS-920 emission spectrophotometers in the UNC EFRC Instrumentation Facility established by the UNC EFRC: Center for Solar Fuels, an Energy Frontier Research Center funded by the U.S. Department of Energy, Office of Science, Office of Basic Energy Sciences under Award Number DE-SC0001011. The authors thank Phil Castellano, Jillian Dempsey, Seth Barrett and Kelsey Brereton for fruitful discussions.

■ REFERENCES

(1) Gray, H. B.; Maverick, A. W. *Science* **1981**, *214*, 1201.
(2) Walter, M. G.; Warren, E. L.; McKone, J. R.; Boettcher, S. W.; Mi, Q.; Santori, E. A.; Lewis, N. S. *Chem. Rev.* **2010**, *110*, 6446.
(3) Lewis, N. S.; Nocera, D. G. *Natl. Acad. Eng.* **2015**, *2*, 43.
(4) Grimes, C. A.; Varghese, O. K.; Ranjan, S. *Light, Water, Hydrogen: The Solar Generation of Hydrogen by Water Electrolysis*; Springer: New York, 2008.
(5) Eckenhoff, W. T.; Eisenberg, R. *Dalton Trans.* **2012**, *41*, 13004.
(6) Fukuzumi, S. *Eur. J. Inorg. Chem.* **2008**, *9*, 1351.
(7) Teets, T. S.; Nocera, D. G. *Chem. Commun.* **2011**, *47*, 9268.
(8) Elgrishi, N.; Teets, T. S.; Chambers, M. B.; Nocera, D. G. *Chem. Commun.* **2012**, *48*, 9474.
(9) Perutz, R. N.; Procacci, B. *Chem. Rev.* **2016**, *116*, 8506.
(10) Pitman, C. L.; Miller, A. J. M. *ACS Catal.* **2014**, *4*, 2727.
(11) Barrett, S. M.; Pitman, C. L.; Walden, A. G.; Miller, A. J. M. *J. Am. Chem. Soc.* **2014**, *136*, 14718.
(12) Suenobu, T.; Guldi, D. M.; Ogo, S.; Fukuzumi, S. *Angew. Chem., Int. Ed.* **2003**, *42*, 5492.
(13) Ziessel, R. *Angew. Chem., Int. Ed. Engl.* **1991**, *30*, 844.
(14) Ziessel, R. *J. Am. Chem. Soc.* **1993**, *115*, 118.
(15) Barrett, S. M.; Slattery, S. A.; Miller, A. J. M. *ACS Catal.* **2015**, *5*, 6320.
(16) Abura, T.; Ogo, S.; Watanabe, Y.; Fukuzumi, S. *J. Am. Chem. Soc.* **2003**, *125*, 4149.
(17) Gabrielsson, A.; van Leeuwen, P.; Kaim, W. *Chem. Commun.* **2006**, *47*, 4926.
(18) (a) Ogo, S.; Kabe, R.; Hayashi, H.; Harada, R.; Fukuzumi, S. *Dalton Trans.* **2006**, 4657. (b) Himeda, Y.; Miyazawa, S.; Onozawa-Komatsuzaki, N.; Hirose, T.; Kasuga, K. *Dalton Trans.* **2009**, 6286. (c) Miller, A. J. M.; Heinekey, D. M.; Mayer, J. M.; Goldberg, K. I. *Angew. Chem., Int. Ed.* **2013**, *52*, 3981. (d) Brewster, T. P.; Miller, A. J. M.; Heinekey, D. M.; Goldberg, K. I. *J. Am. Chem. Soc.* **2013**, *135*, 16022.
(19) Geoffroy, G. L.; Wrighton, M. S. *Organometallic Photochemistry*; Academic Press: New York, 1979.
(20) Wang, W.; Rauchfuss, T. B.; Bertini, L.; Zampella, G. *J. Am. Chem. Soc.* **2012**, *134*, 4525.
(21) Costentin, C.; Dridi, H.; Savéant, J. M. *J. Am. Chem. Soc.* **2014**, *136*, 13727.
(22) Dempsey, J. L.; Brunschwig, B. S.; Winkler, J. R.; Gray, H. B. *Acc. Chem. Res.* **2009**, *42*, 1995.
(23) Collman, J. P.; Wagenknecht, P. S.; Lewis, N. S. *J. Am. Chem. Soc.* **1992**, *114*, 5665.
(24) Collman, J. P.; Ha, Y.; Wagenknecht, P. S.; Lopez, M.-A.; Guilard, R. *J. Am. Chem. Soc.* **1993**, *115*, 9080.
(25) Nicholson, R. S.; Shain, I. *Anal. Chem.* **1964**, *36*, 706.
(26) Pitman, C. L.; Brereton, K. R.; Miller, A. J. M. *J. Am. Chem. Soc.* **2016**, *138*, 2252.
(27) Ladwig, M.; Kaim, W. *J. Organomet. Chem.* **1992**, *439*, 79.
(28) Steckhan, E.; Herrmann, S.; Ruppert, R.; Dietz, E.; Frede, M.; Spika, E. *Organometallics* **1991**, *10*, 1568.
(29) Caix, C.; Chardon-Noblat, S.; Deronzier, A.; Ziessel, R. *J. Electroanal. Chem.* **1996**, *403*, 189.
(30) McCarthy, B. D.; Martin, D. J.; Rountree, E. S.; Ullman, A. C.; Dempsey, J. L. *Inorg. Chem.* **2014**, *53*, 8350.
(31) Turro, N. J.; Chen, J. Y. C.; Sartori, E.; Ruzzi, M.; Marti, A.; Lawler, R.; Jockusch, S.; López-Gejo, J.; Komatsu, K.; Murata, Y. *Acc. Chem. Res.* **2010**, *43*, 335.
(32) Refer to Supporting Information for additional details.
(33) Sandrini, D.; Maestri, M.; Ziessel, R. *Inorg. Chim. Acta* **1989**, *163*, 177.
(34) Connick, W. B.; Geiger, D.; Eisenberg, R. *Inorg. Chem.* **1999**, *38*, 3264.
(35) Keyes, T. E.; O'Connor, C. M.; O'Dwyer, U.; Coates, C. G.; Callaghan, P.; McGarvey, J. J.; Vos, J. G. *J. Phys. Chem. A* **1999**, *103*, 8915.
(36) Singh-Rachford, T. N.; Castellano, F. N. *Coord. Chem. Rev.* **2010**, *254*, 2560.
(37) Vincze, L.; Sandor, F.; Pem, J.; Bosnyak, G. *J. Fluoresc.* **1999**, *9*, 11.
(38) Takayasu, S.; Suzuki, T.; Shinozaki, K. *J. Phys. Chem. B* **2013**, *117*, 9449.
(39) Bock, C. R.; Connor, J. A.; Gutierrez, A. R.; Meyer, T. J.; Whitten, D. G.; Sullivan, B. P.; Nagle, J. K. *J. Am. Chem. Soc.* **1979**, *101*, 4815.

DOI: 10.1021/jacs.6b08701
J. Am. Chem. Soc. 2016, 138, 13509−13512